Research Square

Preprints are preliminary reports that have not undergone peer review.
They should not be considered conclusive, used to inform clinical practice,
or referenced by the media as validated information.

Synthesis of Nb(V) Based MOFs with Benzene-1,3,5-Tricarboxylate As a Catalyst For The Catalytic Transfer Hydrogenation of Furfural to 1,5-Pentanediol: Preliminary Studies

Puput Nursetyani
Sebelas Maret University
Witri Wahyu Lestari
witri@mipa.uns.ac.id

Sebelas Maret University
Asranudin Asranudin
National Research and Innovation Agency (BRIN)
Sri Hastuti
Sebelas Maret University
Wirawan Ciptonugroho
Sebelas Maret University
Fauziyah Azhari
Sebelas Maret University

Research Article

Keywords: Nb-MOFs, Catalytic Transfer Hydrogenation, Solvothermal, Furfural, 1,5-Pentanediol

Posted Date: November 9th, 2026

DOI: https://doi.org/10.21203/rs.3.rs-11373365/v1

License: This work is licensed under a Creative Commons Attribution 4.0 International License.
Read Full License

Additional Declarations: No competing interests reported.

Synthesis of Nb(V) Based MOFs with Benzene-1,3,5-Tricarboxylate As a Catalyst For The Catalytic Transfer Hydrogenation of Furfural to 1,5-Pentanediol: Preliminary Studies

Puput Nursetyani[1], Witri Wahyu Lestari[1,2]*†, Asranudin[3]†, Sri Hastuti[1,2]†, Wirawan Ciptonugroho[2,4]†, and Fauziyah Azhari[1]†

[1] Department of Chemistry, Faculty of Mathematics and Natural Sciences, Universitas Sebelas Maret, Jl. Ir. Sutami No. 36 A Kentingan, Jebres, Surakarta, 57126, Indonesia

[2] Interdiciplinary Research Center for Adsorption and Catalysis, Universitas Sebelas Maret, Jl. Ir. Sutami No. 36 A Kentingan, Jebres, Surakarta, 57126, Indonesia

[3] Research Center for Applied Microbiology, National Research and Innovation Agency (BRIN), Cibinong, Indonesia

[4] Department of Chemistry Education, Faculty of Teacher Training and Education, Universitas Sebelas Maret, Jl. Ir. Sutami No. 36 A Kentingan, Jebres, Surakarta, 57126, Indonesia

*Corresponding author. Email (s): witri@mipa.uns.ac.id;

Contributing authors: pnursetyani@student.uns.ac.id; asra003@brin.go.id , srihastuti71@staff.uns.ac.id; wirawan_ciptonugroho@staff.uns.ac.id; fauziyah617@student.uns.ac.id

†These authors contributed equally to this work.

Abstract

The conversion of biomass into high value-added chemicals has attracted considerable attention as a promising strategy for the development of sustainable energy and materials. Among various biomass-derived platform molecules, furfural is considered a potential feedstock for production of 1,5-Pentanediol via catalytic transfer hydrogenation (CTH). This study investigated the preliminary studies of effects of the synthetic method of Nb-based MOF under solvothermal condition (with and without the presence of modulator) on the physicochemical properties of the materials and catalytic performance toward CTH reaction of furfural to 1,5-Pentanediol. Nb-BTC based MOF were successfully synthesized using $NbCl_5$ as the metal precursor and benzene-1,3,5-tricarboxylate (BTC) as the organic linker. The synthesized materials were characterized by Fourier Transform Infrared (FTIR), X-ray Diffraction (XRD), Field Emission Scanning Electron Microscopy-Energy Dispersive X-ray Spectroscopy (FESEM-EDX), Surface Area Analyzer (SAA), and Thermogravimetric

Analysis (TGA). The catalytic performance of Nb-BTC based MOF was evaluated in the physicochemical properties of the material. The catalytic performance of Nb-BTC based MOF was evaluated in the CTH of furfural using isopropanol as the hydrogenation donor in a batch reactor at 120 °C and 5 bar of N_2 pressure for 4 hours. The catalytic evaluation revealed that the Nb-BTC synthesized via solvothermal with modulator exhibited superior catalytic activity, promoting the selective conversion of furfural toward the formation of 1,5-pentanediol up to 68%. The findings demonstrate that the incorporation of a modulator plays a crucial role in tailoring the catalytic activity of Nb-BTC based MOF catalyst.

Keywords: Nb-MOFs, Catalytic Transfer Hydrogenation, Solvothermal, Furfural, 1,5-Pentanediol

1 Introduction

Metal-organic frameworks (MOFs) are porous materials composed of metal ions or metal-oxide clusters linked by organic ligands—acting as bridging compounds—via bonds to form a three dimensional structure. Over the past two decades, MOFs have garnered significant attention due to advantages such as high surface area, tunable porosity, controllable pore structures, and superior catalytic properties [1]. These characteristics make MOFs promising materials for various applications, including gas separation, adsorption, sensing, drug delivery, and heterogeneous catalyst [2]. In the field of catalyst, MOFs possess active sites in the form of Lewis acid centers derived from vacant orbitals at the metal nodes. Catalytic activity can be enhanced through "defect engineering" a strategy involving the controlled creation of structural defects. The loss of ligands previously coordinated to the metal nodes (missing-linker defects) can generate coordinatively unsaturated metal sites that function as Lewis acid centers, whereas additional groups on the metal nodes can form Brønsted acid sites. Beyond providing active sites, the porous nature of MOFs offers a high surface area and a pore system that facilitates adsorption and the diffusion of reactants toward catalytic sites [3, 4]. Despite their advantages, the performance of MOFs as catalyst in influenced by the specific metals and bridging ligands employes; consequently, the resulting stability and activity vary depending on the specific combination of constituent metals and ligands.

Based on these characterics, various types of MOFs have been developed and applied as catalysts in diverse chemical reactions. Zirconium-based MOFs, such as UiO-66, are known for their high thermal and chemical stability; chromium-based MOFs, such as MIL-101, possess large surface areas and pore volumes; copper-based MOFs, such as HKUST-1, provide active Lewis acid sites; and iron-based MOFs exhibit good activity in various oxidation and reduction reactions [5,6]. The selection of metal ions and organic ligands is a crucial factor in determining the stability and catalytic activity of the resulting MOFs. Among these various MOF types, materials containing metal ions such as Al^{3+}, Cr^{3+}, Zr^{4+}, and Nb^{5+} are known to exhibit good stability in aqueous environments [7]. Niobium (Nb) has attracted particular attention due to its strong Lewis acidity and high resistance to liquid-phase conditions [8, 9]. Furthermore, niobium is selected as a mteal center because of its high oxidation state (Nb^{5+}), which results in high charge density and renders the metal highly oxophilic [9]. These characteristics make Nb(V) a potential active metal center for catalysis, yet its utilization remains relatively limited compared to metals such as Zr, Cr, and Cu. The use of niobium(V) as a metal center in MOFs has been reported by Coelho et al. (2024) through the synthesis of an Nb-MOF based on the terephthalate

(BDC) ligand; this material demonstrated good catalytic activity in the $NaBH_4$ dehydrogenation reaction, achieving a hydrogen yield of 80% [10]. However, H_2BDC is a ditopic linker possessing only two carboxylate groups, resulting in a relatively lower framework connectivity compared to polytopic ligands. Therefore, replacing the H_2BDC ligand with the benzene-1,3,5-tricarboxylate (BTC) ligand is an attractive avenue for development. Benzene-1,3,5-tricarboxylate (H_3BTC) is a tritopic linker possessing three carboxylate groups, enabling the formation of coordination structures with higher connectivity and degrees of cross-linking [11]. These characteristics are expected to enhance the material's physicochemical properties, thereby enabling its application as a catalyst—particularly in the transformation of platform compounds into high-value commercial chemicals.

One potential application of Nb-based MOF catalysts is the conversion of biomass into high-value commercial chemicals. Indonesia possesses immense biomass potential—particularly from agricultural waste such as rice straw, sugarcane bagasse, and coconut husks—generating over 146.7 million tons of biomass is furfural, produced via hemicellulose hydrolysis, notably from sources like coconut coir and tree bark [13]. Furfural is a versatile compound that can be converted into various high-value chemical products, such as furan, furfuryl alcohol, tetrahydrofuran, 1,2-pentanediol, and 1,5-pentanediol [14]. The conversion of furfural to 1,5-pentanediol is a significant area of focus due to the compound's high commercial value, evidenced by a market growth potential of 6.6% per year [14]. According to a Data Bridge Market Research report, the global market for 1,5-pentanediol is projected to reach USD 42 million by 2027 [15]. This compound is widely used in the production of polyurethanes and polyesters, as well as a solvent in the pharmaceutical industry [16]. However, achieving high selectivity in the hydrogenation of furfural to 1,5-pentanediol remains a challenge. Liang et al. (2025) reported a 1,5-pentanediol selectivity of 53.7% during furfural hydrogenation using a Y-modified Co-based catalyst, indicating a continued need to improve selectivity toward the target product [17]. The efficiency of this reaction is significantly influenced by faactors such as the type of catalyst, solvent, reaction temperature, and hydrogen pressure [18]. The use hydrogen gas in conventional hydrogenation requires specialized, expensive equipment and entails high risks [14]. Therefore, there is a need for alternative methods that are safer, more energy-efficient, and sustainable; one such method is catalytic transfer hydrogenation (CTH).

Catalytic transfer hydrogenation (CTH) is a hydrogenation method that utilizes hydrogen donor compounds—such as alcohols—to generate hydrogen in situ via dehydrogenation, thereby eliminating the need for high-pressure hydrogen gas. This approach is considered safer, more more energy-efficient, and more environmentally friendly than conventional hydrogenation [19].

The success of CTH reactions relies heavily on the characteristics of the heterogeneous catalyst employed, particularly the presence of active Lewis and Brønsted acid sites and high thermal and chemical stability [20]. Consequently, MOF-based catalysts offer a promising solution for enhancing efficiency and selectivity in these reactions. However, the use of Nb-MOFs as catalysts for the CTH of furfural to 1,5-pentanediol remains underexplored. Therefore, this study aims to synthesize and characterize an Nb-MOF based on the BTC^{3-} ligand and to evaluate its catalytic performance in the CTH of furfural to 1,5-pentanediol. The findings are expected to contribute scientifically to the understanding of the efficiency and selectivity of Nb-MOF-based catalysts.

2 Experimental

2.1 Materials

All reagents used in this study were of analytical grade and were employed as received, without undergoing any additional purification procedures. Anhydrous niobium chloride ($NbCl_5$, 99.9%), N,N'-dimethylformamide (DMF, 99.8%), 1,5-pentanediol (99%), isopropanol (99.8%), glacial acetic acid (CH_3COOH, 100%) , and ethanol (99.9%) were commercially obtained from Merck, Germany. Trimesic acid (H_3BTC, 99.8%), Furfural (99%) was purchased from Sigma Aldrich and deionized water was supplied by Citosa Kamila Prima.

2.2 Method

The synthesis of Nb-BTC based MOFs was carried out using a solvothermal method with two variations of reaction condition: one without a modulator and another with the addition of an acetic acid as modulator. This synthesis method was modified from a previous study [10, 21]. These two synthetic variations aimed to determine the effect of using a modulator on the physic chemical properties of materials including crystallinity, surface area and porosity, thermal stability, and morphology of the resulting materials.

2.2.1 Synthesis of Nb-BTC based MOFs without a modulator

$NbCl_5$ (0.270 g, 1 mmol) was dissolved in 10 mL of N,N'-dimethylformamide (DMF). Separately, benzene 1,3,5-tricarboxylic acid (H_3BTC, 0.210 g, 1 mmol) was dissolved in 10 mL of N,N'-dimethylformamide (DMF). Each solution was stirred at 500 rpm for 1 hour at room temperature. The two solutions were then mixed and again stirred at 500 rpm for 1 hour at room temperature. The reaction mixture was subsequently transferred to a Teflon-lined autoclave, heated at 130 °C for 24 hours in an oven (Memmert UN30-1060 E7086), and then cooled to room temperature. Unreacted ligand residues were removed by washing with 30 mL of DMF for 1 hour at 90 °C and 30 mL of ethanol for 24 hours at 70 °C, followed by drying at room

temperature to obtain powder Nb-BTC based MOF (without a modulator).

2.2.2 Synthesis of Nb-BTC based MOFs with a modulator

$NbCl_5$ (0.270 g, 1 mmol) was dissolved in 10 mL of a mixture of N,N'-dimethylformamide (DMF) and glacial acetic acid (1:1). Separately, benzene, 1,3,5-tricarboxylic acid (H_3BTC, 0.210 g, 1 mmol) was dissolved in 10 mL of a mixture of N,N'-dimethylformamide (DMF) and glacial acetic acid (1:1). Each solution was stirred at 500 rpm for 1 hour at room temperature. The two solutions were then combined and stirred at 500 rpm for 1 hour at room temperature. The reaction mixture was subsequently transferred to a Teflon-lined autoclave, heated at 130 °C for 24 hours in an oven (Memmert UN30-1060 E7086), and then cooled to room temperature. Unreacted ligand residues were washed with 30 mL of DMF for 1 hour at 90 °C and 30 mL of ethanol for 24 hours at 70 °C, followed by drying at room temperature to obtain solid Nb-BTC based MOF (with the modulator).

2.2.3 Catalytic Test of Nb-BTC for the Catalytic Hydrogen Transfer (CTH) Reaction of Furfural Using a Batch Reactor

Catalytic test of the CTH reaction was conducted using furfural as the substrate and isopropanol as the reagent in a batch reactor setup. The hydrogenation process involved mixing furfural, isopropanol and catalyst in the reactor at 120 °C for 4 hours, with a stirring speed of 500 rpm. During the reaction, N_2 gas was also introduced at a pressure of 5 bar. The resulting reaction mixture was then separated from the catalyst via centrifugation and filtered using a syringe filter. The reaction products were analyzed using a Thermo Scientific TRACE 1310 gas chromatograph equipped with a flame ionization detector (FID). A capillary column coated with 5% phenyl methyl polysiloxane (0.25 mm × 30 m) was used, with nitrogen as the carrier gas. The total run time was 13 min. The injector temperature was maintained at 200 °C, while the oven temperature was initially held at 40 °C for 1 min and then gradually increased to 180 °C over 7 min. The FID temperature was set at 200 °C, with an air flow rate of 300 mL min^{-1}. Additionally, variations in the 5, 10, and 20 wt.% catalyst mass percentage and the reagent-to-substrate ratio 1:10 and 1:20 were investigated.

GC analysis was performed to determine the retention times of the CTH furfural reaction products, enabling qualitative analysis through comparison with standard retention times. Additionally, the GC analysis aimed to determine the peak area of each compound, allowing for the calculation of catalytic activity. Catalytic activity parameters—namely conversion, yield, and selectivity—was calculated using these equations 1-3 [22].

$$\text{Conversion (\%)} = \frac{C\ initial\ furfural - C\ final\ furfural}{C\ initial\ furfural}\ x\ 100\% \quad \text{.....(1)}$$

$$\text{Yield (\%)} = \frac{C\ final\ 1,5-pentanadiol}{C\ initial\ furfural}\ x\ 100\% \quad \text{.....(2)}$$

$$\text{Selectivity (\%)} = \frac{C\ final\ 1,5-pentanadiol}{C\ furfural\ reacted}\ x\ 100\% \quad \text{.....(3)}$$

2.2.4 Materials Characterization

The synthesized materials were analysed using an Expert PAN analytical diffractometer over a 2θ range of 5–90°, using Cu Kα radiation (λ = 1.5406 Å) to investigate the crystallinity and phase purity. The shifts and changes in functional groups occurring during the synthesis were monitored using Fourier-transform infrared (FTIR) spectroscopy (Shimadzu IR Prestige-21) in the range of 4000–400 cm^{-1} using KBr pellets. Thermal stability of the materials was measured using Differential Thermal/Thermo Gravimetry Analysis (TGA/DTA) (Leco TGA701, with heating rate 10 ^oC/minute, in temperature range 30-900 ^oC). Morphology, textural analysis, and elemental composition of the materials were observed using Field Emission Scanning Electron Microscopy (FESEM-EDX) (JSM-6510LA). Nitrogen sorption isotherm measurement was conducted on BELSORP MA XG with the sample previously activated under vacuum at 150 °C for 24 hours.

3 Results and Discussion

3.1 Materials Synthesis

Nb-BTC based MOFs were successfully synthesized from $NbCl_5$ and H_3BTC using the solvothermal method, with and without the addition of acetic acid as a modulator. The formation of a white to slightly yellowish-white precipitate indicated the successful formation of the Nb-BTC based MOFs coordination polymer. The coordination between the carboxylate groups of the BTC linker and the Nb(V) metal centers represents a crucial step in determining the structure and stability of the resulting framework [10]. The addition of acetic acid was employed to regulate the nucleation and crystal growth through competitive coordination with Nb(V) centers. The resulting Nb-BTC-NM (non modulator) and Nb-BTC-M (with acetic acid as modulator) were obtained as white to slightly yellowish-white powders, with yields of 47.70% and 47.50%, respectively (Figure 1a and 1b). The similar yields obtained for both materials indicate that the addition of acetic acid did not substantially affect the overall synthesis yield.

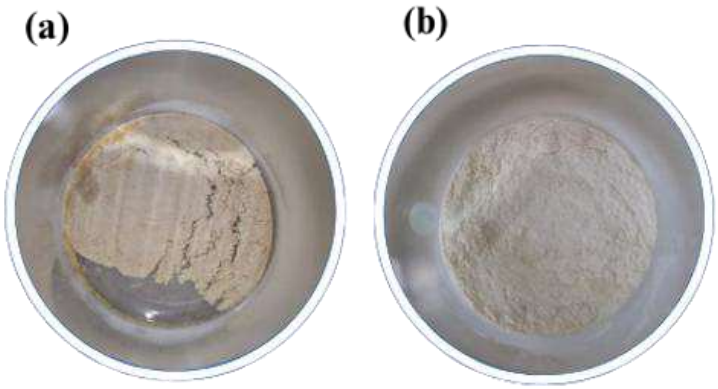


Fig. 1 Synthesized materials (a) Nb-BTC-NM (b) Nb-BTC-M

3.2 Material Characterization

FTIR analysis was conducted to evaluate the successful synthesis of Nb-BTC based on changes in the characteristic absorption band of functional groups and the appearance of new bands compared with BTC^{3-} ligand. Figure 2a show the FTIR spectra of BTC^{3-} ligand and the synthesized of Nb-BTC based MOFs. The spectrum of BTC exhibited an absorption band at 1720 cm^{-1}, which is assigned to stretching vibration of the carboxylic acid group (-COOH). After synthesis, this band changed to two distinct absorptions peaks at 1550 and 1368 cm-1 for the Nb-BTC-M and 1548 and 1369 cm^{-1} for Nb-BTC-NM, corresponding to asymmetric and symmetric stretching vibrations of the carboxylate groups (COO^-). The changes in these absorption bands are associated with the deprotonation of the carboxyl groups and their coordination with Nb(V) centers, indicating the involvement of BTC^{3-} in the formation of the Nb-BTC based MOF framework [10]. The O-H stretching region of BTC^{3-}, observed at 2554-3100 cm^{-1}, also showed a shift after framework formation, while the aromatic C= C stretching band at 1605 cm^{-1} was retained at 1607 cm^{-1} for Nb-BTC-M and 1615 cm^{-1} for the Nb-BTC-NM, suggesting that the aromatic structure of BTC remaining intact. Moreover, new absorption bands appeared at 582 and 580 cm^{-1} for the Nb-BTC-M and Nb-BTC-NM, respectively, which are assigned to Nb-O vibrations [10]. The presence of these Nb-O bands, together with changes in the carboxylic and O-H regions, provides further evidence for the formation of coordination interactions between Nb(V) and carboxylate moieties of BTC in both Nb-BTC based MOFs.

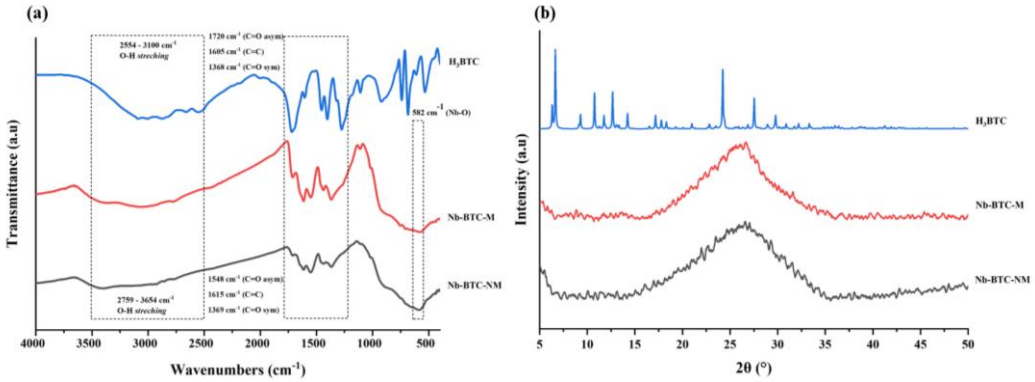


Fig. 2 (a) FTIR spectra of Nb-BTC-NM and Nb-BTC-M, compared with the H_3BTC (b) X-Ray diffactograms of Nb-BTC-NM and Nb-BTC-M, compared with the H_3BTC.

Figure 2b present the X-ray diffraction pattern of BTC3- and the synthesized Nb-BTC based MOFs. The BTC^{3-} ligand exhibited several sharp diffraction peaks in the 2θ range of 5-30 °, indicating highly crystalline structure. After synthesis using the Nb(V) precursor, the characteristic diffraction peaks of BTC^{3-} were no longer observed in either Nb-BTC-M or Nb-BTC-NM. This suggests that the linker underwent structural changes through coordination with Nb(V) center and formed a new phase distinct from the organic precursor [23]. The Nb-BTC based MOFs indicating a low degree of long-range structural ordering and suggesting semi-crystalline to amorphous characteristics. Although the lower crystallinity indicated a less ordered structure, this characteristic may be beneficial for catalytic application by providing grater accessibility to metal centers and potential active sites for adsorption, diffusion of substrate, and catalytic reactions [24]. Therefore, the synthesized Nb-BTC baed MOFs, depsite their semi-crystalline to amorphous characteristics, remain promising materials for heterogeneous catalytic applications.

The nitrogen adsorption-desorption isotherms in Figure 3a show a Type I isotherm for the Nb-BTC-M and Nb-BTC-NM. According the IUPAC classification, this type of isotherm indicates the presence of microspores. Both materials also show a separation between the adsorption and desorption branches, forming a hysteresis loop similar to the H3 type, which is generally associated with slit-shaped pores and may result from particle aggregation. The pora size distribution shown in Figure 3b indicates that the Nb-BTC based MOFs have a non-uniform pore size distribution, with pores ranging from the micropore (2 nm) to mesopore region (2-5 nm) [25]. As presented in Table 1. The Nb-BTC-M exhibits a higher BET surface area of 189.89 m^2/g^{-1} than the Nb-BTC-NM, which has a BET surface area of 79.53 m^2/g^{-1}. The pore volume and pore diameter also show higher values for the Nb-BTC-M, as presented in Table 1. This improvement in textural properties can be attributed to the addition of acetic

acid during synthesis, which can influence the nucleation and crystal growth processes, resulting in better pore accessibility. The hogher surface area and porosity may facilitate the adsorption and diffusion of reactants within the material during the catalytic reaction.

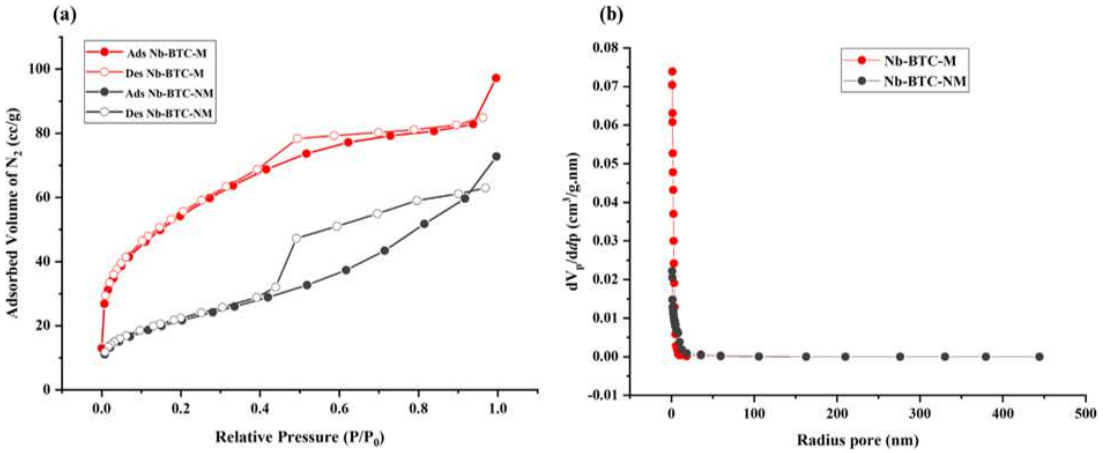


Fig. 3 (a) N_2 adsorption-desorption isotherm plot (b) pore radius distribution of Nb-BTC-M and Nb-BTC-NM

Table 1. Surface area BET, volume pore, and diameter pore Nb-BTC based MOFs synthesized

Material	Surface area BET (m^2/g^{-1})	Pore Volume (cc/g)	Pore Diameter (nm)
Nb-BTC-M	189.89	0.166	1.190
Nb-BTC-NM	79.53	0.118	1.045

FESEM analysis of the materials are shown in Figure 4 revealed that the synthesized Nb-BTC based MOFs predominantly exhibited an irregular flake-like morphology. At higher magnification, Nb-BTC based MOFs also showed white spots distributed across the particle surfaces, which may be associated with particle agglomeration and size of the resulting materials. Nb-BTC-M exhibited an average particle size of 2.88 ± 0.133 µm and Nb-BTC-NM showed a smaller average particle size of 2.40 ± 0.825 µm. The addition of acetic acid resulted in larger particles size compared with the result of non-modulator synthesis approach. The larger particle size observed for the Nb-BTC-M may be attributed to the role acetic acid as a modulator, which competes with the BTC^{3-} linker for coordination with the Nb(V) centers, thereby reducing the nucleation rate and allowing further particle growth [3].

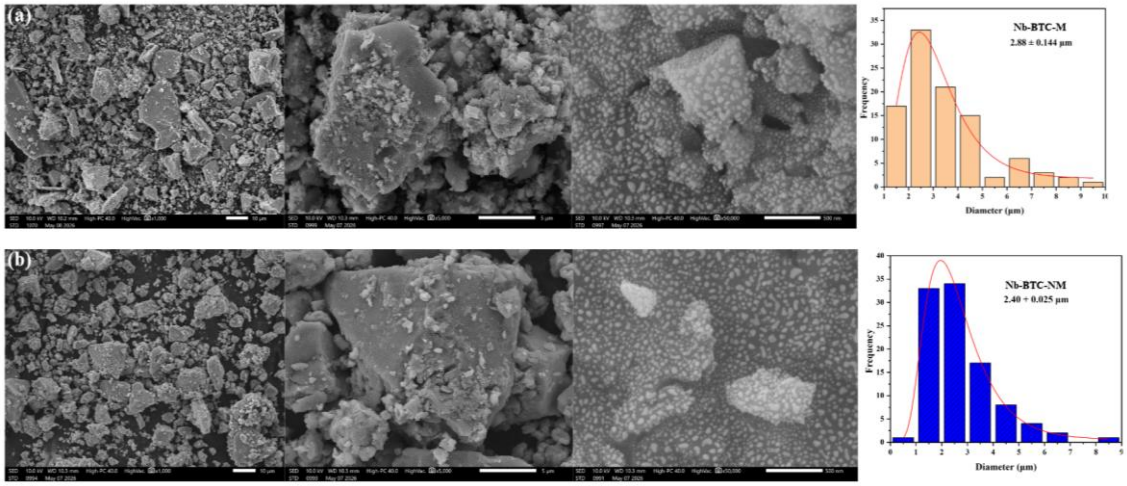


Fig. 4 FESEM images of the materials at 1000x, 5000x and 50.000x magnification and particle distribution (a) Nb-BTC-M (b) Nb-BTC-NM

Table 2. Element composition of synthesized Nb-BTC based MOFs

Material	C (%)	O (%)	Nb (%)
Nb-BTC-M	30.22	44.80	24.99
Nb-BTC-NM	29.64	50.34	20.02

Energy dispersive X-ray (EDX) analysis was performed to qualitatively identify the elemental composition of Nb-BTC based MOFs, as shown in Figure 5. The EDX spectra and elemental mapping confirmed detected in both materials were present within relatively similar ranges, indicating that the use of acetic acid during synthesis did not alter the main elemental composition of the materials. Although variations in elemental composition were observed between the Nb-BTC-M and Nb-BTC-NM, these differences were relatively small and did not indicate a significant change. The elemental compositions of both Nb-BTC based MOFs in terms of atomic percentage (At %) are presented in Table 3. The EDX results confirmed the presence of C, O, and Nb in both materials, supporting the formation of Nb-BTC based MOFs with similar elemental compositions.

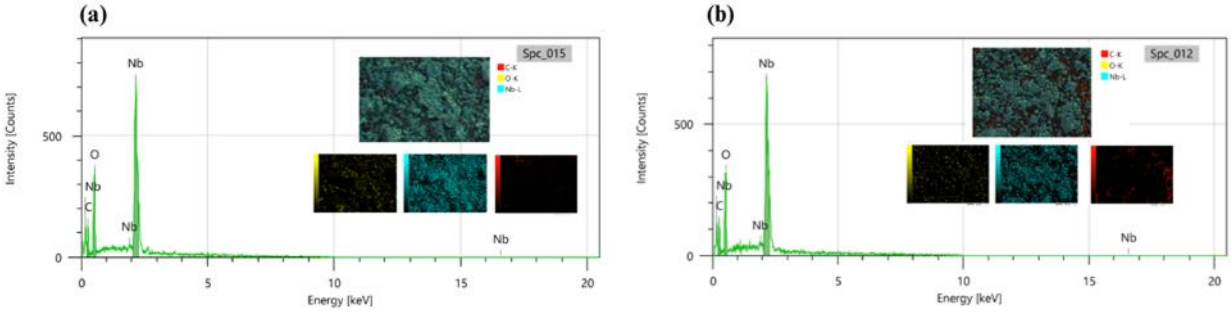


Fig. 5 EDX spectra of the synthesized material (a) Nb-BTC-M (b) Nb-BTC-NM

Thermogravimetric analysis (TGA) was performed to evaluate the thermal stability of the synthesized Nb-BTC based MOFs. The thermograms shown in Figure 6 exhibit three stages of mass change. The first stage, occurring at RT - 200 °C is associated with the removal of water molecules and volatile components present within the pores, with remaining masses of 31.33% for Nb-BTC-M and 28.36% for Nb-BTC-NM. The second stage, observed at 200 – 450 °C is attributed to the removal and decomposition of residual DMF and acetic acid. At temperatures above 500 °C, the remaining mass decrease is associated with the decomposition of the BTC linker and subsequent collapse of the Nb-MOF framework.

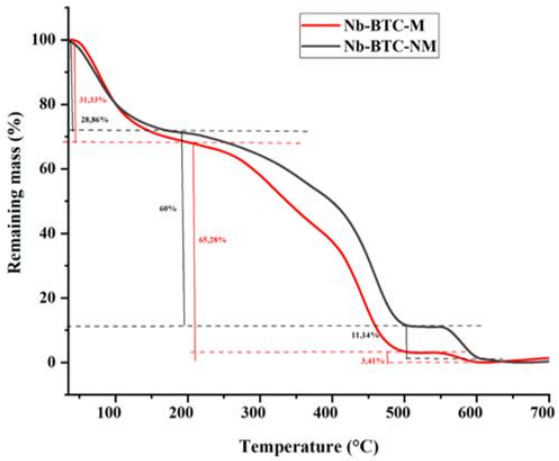


Fig. 6 Thermogram of synthesized materials (both for Nb-BTC-M and Nb-BTC-NM)

3.2 Catalytic Test

The catalytic activity of obtained Nb-BTC based MOFs was evaluated in the catalytic transfer hydrogenation (CTH) of furfural to 1,5-pentanediol using isopropanol as the hydrogen donor. The reaction was conducted in a batch reactor at 120 °C, under 5 bar N_2 pressure, for 4 hours. Quantitative analysis was performed using GC-FID based on calibration curves of furfural and 1,5-pentanediol, with correction factor (cf) values of 0.5155 and 0.400, respectively (calibration curves in Figure S1; GC-FID chromatograms of catalytic test variations in Figures S2-S4). GC-MS analysis confirmed the formation of the target product, with a distinct peak at a retention time of 5.97 min identified as 1,5-pentanediol (chromatogram in Figure S5). Figure 7a shows that increasing the catalyst loading from 5 wt% to 10 wt% enhanced the conversion and selectivity from 5% and 41% to 14% and 68%, respectively. This improvement indicates that increasing the amount of catalyst provides more accessible active sites, thereby facilitating the reaction. However, further increasing the catalyst loading to 20 wt% resulted in a decrease in catalytic performance. The decrease may be associated with catalyst particle agglomeration and increased mass-transfer limitation, which restrict the accessibility of reactants to the active sites [20]. Subsequently, the effect of the furfural to

isopropanol ratio was investigated, where isopropanol acts as a hydrogen donor through a Meerwein-Ponndorf-Verley (MPV) type mechanism. As shown in Figure 7b, the catalytic performance was optimal at afurfural to isopropanol ratio of 1:10. Increasing the isopropanol ratio from 1:10 to 1:20 significantly decreased the selectivity from 64% to 4%. An excess of isopropanol may reduce the concentration of furfural near the catalyst surface through a dilution effect, thereby weakening the effective interaction between furfural and the active sites [26]**.** Therefore, a furfural to isopropanol ratio of 1:10 was selected as the optimum condition, providing a suitable balance between hydrogen donor availability and furfural concentration while resulting in higher yield and selectivity toward the target product.

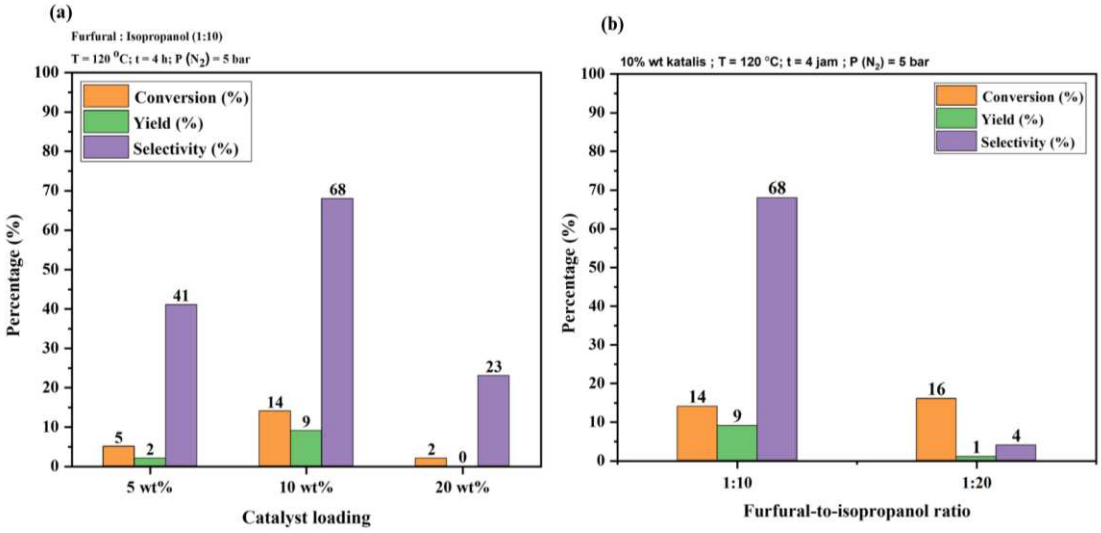


Fig. 7 Catalytic performance of Nb-BTC-M (a) catalyst loadings of 5, 10, and 20 wt%; (b) furfural-to-isopropanol ratio of 1:10 and 1:20

After the optimum reaction conditions were determined, the effect of acetic acid modulation on the catalytic performance was investigated. Figure 8 show the effect of acetic acid addition during the synthesis of Nb-BTC on its catalytic performance. The reaction without a catalyst was used as a control experiment and resulted in 28% furfural conversion without the formation of 1,5-pentanediol. The conversion observed in the absence of a catalyst indicates that furfural can undergo transformation under the reaction conditions, but the reaction does not processed selectively toward the target product. In contrast, Nb-BTC-NM resulted in 19% conversion, 4% yield and 21% selectivity, whereas Nb-BTC-M exhibited 14% conversion, 9% yield and 68% selectivity. The enhanced selectivity indicates that the use of acetic acid as a modulator during synthesis can influence the material characteristics, thereby promoting a more selective conversion pathway of furfural toward the target product. The modulator may affect the nucleation and crystal growth processed during framework formation. This performance can be associated with favorable physicochemical properties, including a high surface area (189.89

m^2g^{-1}), larger pore volume (0.166 cm^3g^{-1}), larger pore diameter (1.190 nm) and higher Nb content (24.99%). These characteristics play an important role in determining the accessibility of reactant molecules to the active sites [4]. Therefore, the higher selectivity of Nb-BTC-M toward 1,5-pentanediol can be associated with its physicochemical characteristics, which facilitate the adsorption and diffusion of reactants during the reaction.

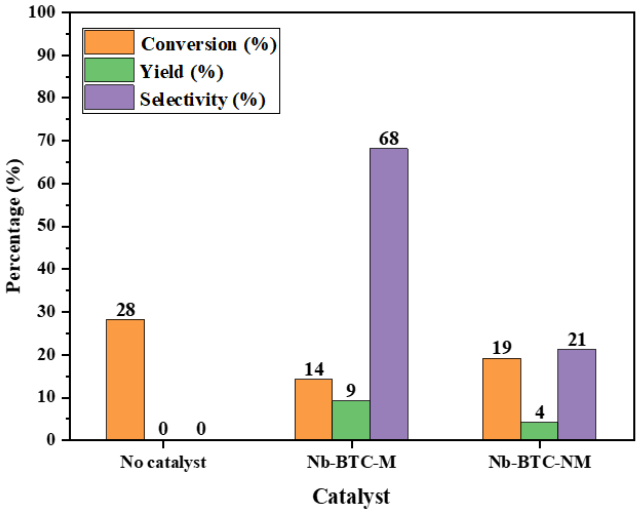


Fig. 8 Catalytic performance of Nb-BTC-M and Nb-BTC-NM compared with the absence of catalyst

The catalytic performance of the optimized Nb-BTC based MOFs was subsequently compared with representative catalysts reported for the conversion of furfural to 1,5-pentanediol (Table 3). The Nb-BTC-M exhibited a high selectivity up to 68%, which was higher than those reported for Pt-Co-Mg-A 1 (47%), Ni-Co-Al (48%), and Ni/CoAlOx (42.9%). This result demonstrates the ability of Nb-BTC-M to direct the conversion of furfural toward 1,5-pentanadiol while suppressing the formation of side products. This performance indicates that the Nb active sites within the MOF framework contribute to the reaction to the reaction pathway toward the desired diol product, while modification with acetic acid may influence the chemical enviroment and accessibility of the active sites, thereby enhancing selectivity. In addition to the structural factors, the catalytic performance of Nb-BTC-M is also influenced by the reaction conditions, as the formation of 1,5-pentanediol involves several steps, including carbonyl hydrogenation, ring hydrogenation, and furan ring opening. Therefore, the characteristics of the active sites and the operating parameters play important roles in determining the product distribution.

Table 3. Comparison of catalytic performance for the conversion furfural to 1,5-pentanediol with previously reported catalysts.

Catalyst	Reaction conditions	Conversion (%)	Yield (%)	Selectivity (%)	Reference
Ru-Sn/ZnO	140 °C; 3 MPa H_2; 6 h; solvent isopropanol	100	12.4	-	[27]
Pt-Co-Mg-Al	150 °C; 3 MPa H_2; 4 h; solvent isopropanol	100	-	47	[28]
Ni/CoAlOx	150 °C; 1.5 Mpa H_2; 6 h; solvent isopropanol	100	-	42.8	[29]
Co/Y	150 °C; 4 Mpa H_2; 5 h; solvent isopropanol	-	-	53.7	[30]
2Pt@Co^{2+}/MMO	150 °C; 3 Mpa H_2; 4 h; solvent isopropanol	100	47	47	[28]
CoAlO-r700	150 °C; 3 MPa H_2; 8 h	-	30	-	[31]
Ni-Co-Al	160 °C; 3 MPa H_2; 6 h; solvent etanol	100	-	48	[15]
ZIF-8	160 °C; 6 MPa H_2; 5 h	100	-	25.4	[32]
Nb-BTC-M	120 °C; 5 bar N_2; 4 h; solvent isopropanol	14	9	68	This study

Nb-BTC-NM	120 °C; 5 bar N2; 4 h; solvent isopropanol	19	4	21	This study

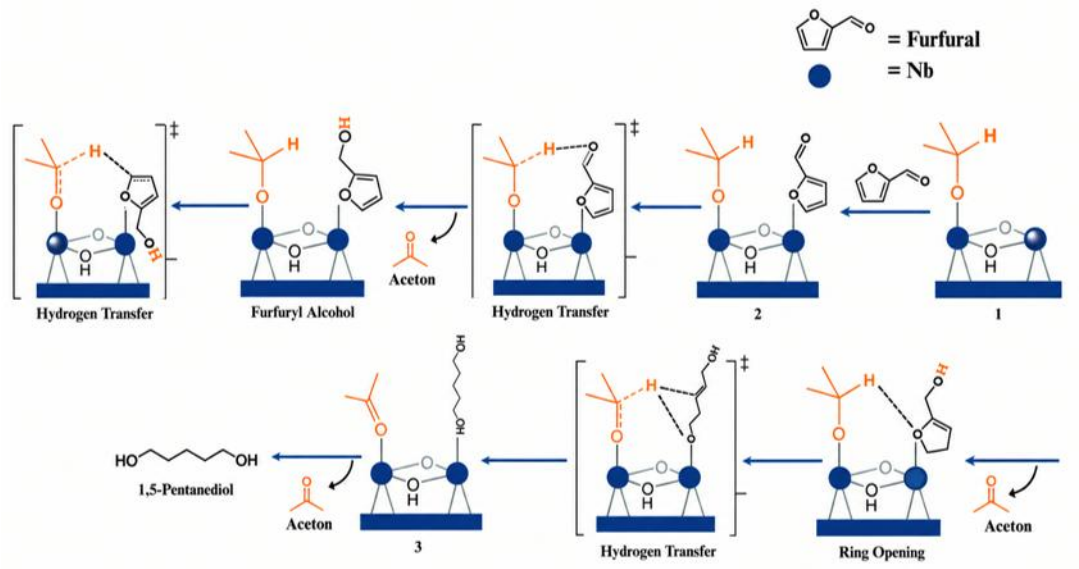


Fig. 9 Proposed reaction mechanism of furfural to 1,5-pentanediol catalysed by Nb-BTC based MOFs

The proposed mechanism for the catalytic transfer hydrogenation of furfural using Nb-BTC based MOFs is illustrated in Figure 9. The reaction proceeds through the dehydrogenation of isopropanol on the Nb-BTC based MOFs surface, producing acetone as a by-product along with active hydrogen species. These species are subsequently transferred to furfural. In the first step, the carbonyl group furfural is hydrogenated to form furfuryl alcohol. The activation of the carbonyl group is proposed to occur through the interaction between the oxygen atom of furfural and the Lewis acid from Nb centers. Subsequently, the furan ring in furfuryl alcohol undergoes hydrogenation and ring opening, resulting in the formation of an open-chain intermediate. This intermediate then undergoes further hydrogenation to produce 1,5-pentanediol. The Nb centers are proposed to play a role in activating oxygen-containing intermediates and facilitating C-O bond cleavage during the ring opening process. In addition to the main reaction pathway, incomplete ring opening, alternative C-O bond cleavage, and excessive hydrogenation or hydrogenolysis may promote the formation of by-products, consequently decreasing the selectivity toward 1,5-pentanediol.

4 Conclusions

Nb-BTC based MOFs was successfully synthesized and applied as a catalyst for the catalytic transfer hydrogenation (CTH) furfural to 1,5-pentanediol. FTIR characterization confirmed the formation of Nb-O bonds, while XRD analysis revealed a semi-crystalline or amorphous structure and morphology showed irregular flakes. Nb-BTC-M exhibited the highest catalytic activity under the optimum reaction conditions, 10 wt% catalyst loading, a furfural ratio 1:10, 120 °C, N_2 pressure of 5 bar and 4 hours, achieving a selectivity of 68% toward 1,5-pentanediol. This catalytic performance was supported by the physicochemical properties of Nb-MOF, including high surface area 189.89 $m^2\ g^{-1}$, pore volume 0.166 $cm^3\ g^{-1}$, pore diameter 1.190 nm, and Nb content 24.99%. Further research directed to optimized synthetic condition of Nb-BTC based MOFs including reaction, temperature, solvent variation, stoichiometry between linker and the metals, as well as synthetic method such as microwave assisted synthesis, mechanochemical synthesis, electrochemical synthesis etc. Parameters in catalytic test such as temperature, reaction time, pressure and solvent need also to be optimized. However the results in this preliminary studies will open the gate in employing Niobium based MOF as catalyst in the catalytic transfer hydrogenation in the transformation of organic compound into high added value product chemicals.

Acknowledgements

This research was supported by Universitas Sebelas Maret (UNS) under scheme Indonesian Research Collaboration (Scheme B) project number 648.1/UN27.22/PT.01.03/2026. We would like also to acknowledge BRIN for the materials characterization through ELSA access.

Declarations

Funding

This study was funded by Indonesian Research Collaboration (Scheme B) project number 648.1/UN27.22/PT.01.03/2026 with partner Universitas Negeri Malang (UM), Research Center for Nanotechnology Systems, National Research and Innovation Agency (BRIN), and Lambung Mangkurat University (ULM).

Competing Interests

The authors have no relevant financial or non-financial interests to disclose.

Ethics approval

Not applicable.

Consent to participate

Not applicable.

Consent for publication

Not applicable.

Availability of data and materials

Not applicable.

Code availability

Not applicable.

Author Contributions

Conceptualization: Witri Wahyu Lestari; Methodology: Puput Nursetyani; Formal analysis and investigation: Puput Nursetyani; Writing - original draft preparation: Witri Wahyu Lestari, Puput Nursetyani; Writing - review and editing: Witri Wahyu Lestari, Sri Hastuti, Wirawan Ciptonugroho, Fauziyah Azhari ; Funding acquisition: Witri Wahyu Lestari; Resources: Witri Wahyu Lestari; Supervision: Witri Wahyu Lestari, Sri Hastuti, Wirawan Ciptonugroho: Analysis, Methodology, Writing - review and editing: Asranudin.

References

1. Y. Wen, P. Zhang, V. K. Sharma, X. Ma, H.C. Zhou, Cell Rep. Phys. Sci. 2, 100348 (2021)
2. D.S.R. Khafaga, M.T. El-Morsy, H. Faried, A.H. Diab, S. Shehab, A.M. Saleh, G.A.M. Ali, RSC Adv. 14, 30201 (2024).
3. X. Feng, H.S. Jena, C. Krishnaraj, K. Leus, G. Wang, H. Chen, C. Jia, P. Van Der Voort, ACS Appl. Mater. Interfaces. 13, 60715 (2021).
4. F. Llabres i Xamena, J. Gascon (eds.), *Metal Organic Frameworks as Heterogeneous Catalysts* (The Royal Society of Chemistry, 2013).
5. C.E.S. Ferreira, S.S. Balula, L. Cunha-Silva, Compounds 4, 315 (2024).

6. J.N. Hall, P. Bollini, React. Chem. Eng. 4, 207 (2019)
7. A.H. Chughtai, N. Ahmad, H.A. Younus, A. Laypkov, F. Verpoort, Chem. Soc. Rev. 44, 6804 (2015)
8. H.N. Pham, Y.J. Pagan-Torres, J.C. Serrano-Ruiz, D. Wang, J.A. Dumesic, A.K. Datye, Appl. Catal. A Gen. 397, 153 (2011)
9. R. Rodrigues, N. Isoda, M. Gonçalves, F.C.A. Figueiredo, D. Mandelli, W.A. Carvalho, Chem. Eng. J. 198–199, 457 (2012)
10. L.O. Coelho, G.H. Sperandio, R. Chagas da Silva, R.P. Lopes Moreira, J.R. de Jesus, Processes 12, 2342 (2024)
11. F. Lo Presti, A. Borzì, A.L. Pellegrino, P. Rossi, P. Paoli, G. Malandrino, Results Chem. 4, 100640 (2022)
12. R.P. Primadanty, Parahyangan Econ. Dev. Rev. 2, 136 (2024)
13. Q. Zhou, A. Ding, L. Zhang, J. Wang, J. Gu, T.Y. Wu, X. Gu, L. Zhang, Fuel Process. Technol. 255, 108063 (2024)
14. K. Huang, Z.J. Brentzel, K.J. Barnett, J.A. Dumesic, G.W. Huber, C.T. Maravelias, ACS Sustainable Chem. Eng. 5, 4699 (2017)
15. R.G. Kurniawan, N. Karanwal, J. Park, D. Verma, S.K. Kwak, S.K. Kim, J. Kim, Appl. Catal. B Environ. 320, 121971 (2023)
16. Z. Yang, J. Zhang, G. Qian, X. Duan, X. Zhou, Green Chem. Eng. 2, 158 (2021)
17. Y. Liang, J. Zuo, Z. Cai, W. Huang, J. Lin, Z. Liu, Ind. Eng. Chem. Res. 64, 7220 (2025)
18. H.W. Wijaya, T. Sato, H. Tange, T. Hara, N. Ichikuni, S. Shimazu, Chem. Lett. 46, 744 (2017)
19. T. Wang, J. Du, Y. Sun, X. Tang, Z.-J. Wei, X. Zeng, S.-J. Liu, L. Lin, Chin. Chem. Lett. 32, 1186 (2021)
20. Y. Wang, P. Prinsen, K.S. Triantafyllidis, S.A. Karakoulia, A. Yepez, C. Len, R. Luque, Chem Cat Chem 10, 3459 (2018)
21. F. Azhari, D.W.T. Wulansari, W. Ciptonugroho, W.W. Lestari, A. Fitriyaningsih, U.S.F. Arrozi, Y.P. Budiman, Res. Chem. Intermed. 50, 5755 (2024)
22. P. Gómez-López, M. Murat, J.M. Hidalgo-Herrador, C. Carrillo-Carrión, A.M. Balu, R. Luque, D. Rodríguez-Padrón, Catalysts 11, 526 (2021)
23. Y. Wu, M.I. Breeze, G.J. Clarkson, F. Millange, D. O'Hare, R.I. Walton, Angew. Chem. Int. Ed. 55, 4992 (2016)
24. Y. Zhang, X. Yu, Y. Hou, C. Liu, G. Xie, X. Chen, Mol. Catal. 555, 113851 (2024)
25. M. Thommes, K. Kaneko, A.V. Neimark, J.P. Olivier, F. Rodriguez-Reinoso, J. Rouquerol, K.S.W. Sing, Pure Appl. Chem. 87, 1051 (2015)

26. H. Chen, H. Ruan, X. Lu, J. Fu, T. Langrish, X. Lu, Mol. Catal. 445, 94 (2018)
27. P.P. Upare, Y. Kim, K.R. Oh, S.J. Han, S.K. Kim, D.Y. Hong, M. Lee, P. Manjunathan, D.W. Hwang, Y.K. Hwang, ACS Sustainable Chem. Eng. 9, 17242 (2021)
28. A. Barranca, I. Gandarias, P.L. Arias, I. Agirrezabal-Telleria, Catal. Lett. 153, 2018 (2023)
29. Q. Shen, Y. Li, F. Wang, X. Zhang, Z. Zhang, Z. Zhang, Y. Yang, C. Bing, X. Fan, J. Zhang, X. He, Mol. Catal. 556, 113919 (2024)
30. Y. Liang, J. Zuo, Z. Cai, W. Huang, J. Lin, Z. Liu, Ind. Eng. Chem. Res. 64, 7220 (2025)
31. L. Gavilà, A. Lähde, J. Jokiniemi, M. Constanti, F. Medina, E. del Río, M. Tichit, M.G. Álvarez, Chem Cat Chem 11, 4944 (2019)
32. Z. Chen, J. Chen, Y. Li, Chin. J. Catal. 38, 1108 (2017)

Supplementary Files

This is a list of supplementary files associated with this preprint. Click to download.

- gaphicalabstract.png
- SupplementaryNbBTCMaterials.docx